6 Observer independent acquisition of cardiac MR short-axis views

Boudewijn P.F. Lelieveldt, Rob J. van der Geest, Hildo J. Lamb, Hein W.M. Kayser, Johan H.C. Reiber
Submitted.

Abstract

Purpose: To develop an automated, observer independent acquisition planning method for short-axis, multi-slice multi-phase cardiac MR imaging studies.

Materials and methods: From twenty patients and two volunteers, multi-slice, multi-phase short-axis MR images were acquired by manual scan planning on a series of localizers (or scout views) following a standard LV function protocol. In addition, the position and spatial orientation of the short-axis image volume were fully automatically calculated by matching a deformable model of the thorax to three-plane localizers.

Results: To assess the accuracy and reproducibility of the automated method as compared to manual scan planning, in each study the angle between the reference geometric LV long axis and the short-axis image normal vector was calculated for both the manual and the automated planning procedure. The error (mean ± s.d.) by the automated method (12.2 ± 6.8 degrees) was not statistically different from the one by the manual scan planning (9.7 ± 5.8 degrees). The quality and image content of the automatically scanned image volumes were comparable to those obtained by manually planned short-axis volumes.

Conclusions: The automated planning method provides a uniform, objective method to fully automatically acquire a set of multi-slice, multi-phase short axis cardiac MR images, without requiring any user interaction or expert knowledge.

6.1 Introduction

Magnetic Resonance Imaging is an excellent tool to assess global and regional left ventricular (LV) function, and is now considered to be the ‘gold standard’ for analysis of, for

example, ejection fraction and ventricular volumes [1]. In particular multi-slice, multi-phase short-axis cardiac MR-images are most suitable to assess left ventricular function without any assumptions about LV geometry [2-11]. However, to plan these scans currently requires substantial insight in cardiac anatomy. Many operators have difficulties in learning to plan the short-axis views in a reproducible manner.

Recently, image analysis tools were introduced towards the automated planning of the short-axis view, thereby potentially reducing operator interaction to a minimum [12-14]. The purpose of the present study therefore, was to investigate, following objective and reproducible criteria, if and by how much the operator interaction can be reduced using an automated technique for the definition of the scan volume for a short-axis cardiac MR set. The basic principle of this approach is based on matching a digital atlas model of the thorax to a set of scout views or localizers. The set of required geometric transformations can subsequently be applied to project the position and orientation of the LV long axis from the model subject on the scout views. Based on these parameters, we have investigated whether the automatic definition of the short-axis image volume can be realized directly from the scout views, where the three-dimensional angle of the LV long axis defines the orientation of the image set. If this would be succesful, then it would provide an objective automatic tool to plan short-axis images, and it would eliminate the necessity to acquire supporting long-axis views used in the current scan planning procedure.

6.2 Materials & methods

Manual short-axis scan planning

To compare the accuracy and reproducibility of the automated planning method with the accuracy as currently achieved on a standard MR system in routine clinical practice, 20 patient examinations were collected retrospectively. No gender/age selection was performed, and patients were selected suffering from various cardiac pathologies (myocardial infarctions (n=14), cardiomyopathies (n=3), congenital anomalies (n=1), arrhythmia (n=1), LV aneurysms (n=1)). In addition, two healthy subjects were scanned according to the automatic procedure; subsequently the scan was repeated using the manual scan planning protocol by an independent expert.

The MR studies were performed on a standard 1.5-T MR imaging system (Philips Gyroscan NT 1.5, Best, the Netherlands). The patient studies were planned by different scanner operators following a standardized cardiac function MR protocol, which is routinely applied in our center to plan short-axis examinations. For technical details see [11]. According to this protocol, patient studies minimally consist of four image sets per patient:

1) a set of cardiac gated, non breathheld scout views acquired following a multistack protocol (9 coronal/9 sagittal/9 transversal images, slice thickness 10 mm, slice gap 1 mm, FOV 450×450 mm, Turbo Field Echo pulse sequence, flip angle 20 degrees, repetition time 8 ms, echo time 4 ms.)

2) a cardiac gated vertical long axis view: planned manually on a transverse slice in the scout views, in a plane parallel to the Cranial-Caudal scanner axis and the LV long axis, and through the LV apex (FFE-EPI, repetition time equal to the RR interval, echo time 11 ms, prospective gating, breathheld in end-expiration, slice thickness 8 mm, reduced FOV 400×237)
3) a four chamber view: planned on the vertical long axis view, and acquired as a plane positioned through the apex, oriented perpendicular to the vertical long axis view and parallel to the LV long axis as seen in the vertical long axis view (FFE-EPI, repetition time equal to the RR-interval, echo time 11 ms, prospective gating, breathheld in end-expiration, slice thickness 8 mm, reduced FOV 400×237 mm).
4) a multi-slice, multi-phase gated short-axis cardiac MR set, planned perpendicular to the 4 chamber view through the apex and perpendicular to the LV long axis. (FFE-EPI, repetition time equal to the RR-interval, echo time 11 ms, prospective gating, breathheld in end-expiration, slice thickness 10 mm, slice gap 1 mm, reduced FOV 400×237 mm).

Automated scan planning

In previous work [12-14], we have described a three-dimensional deformable atlas matching method for the thorax, by which a thoracic MR-set can be fully automatically segmented into the lungs, heart and cardiac ventricles. The model matching procedure results in a set of geometric transformations, which define a one-to-one mapping between the model's thoracic anatomy and that of a patient/volunteer. Anatomical and pathological variations in organ shapes and dimensions are described in variations in size, position and orientation of the different thoracic organs in the thorax with respect to each other. When the model has been fully aligned with the image set, the approximate locations of the boundaries of the heart, cardiac ventricles, right lung and left lung are known. The modeling and matching procedure has been validated in normal subjects [12,13] and in patients [14], and was shown to be robust with respect to noise and initial model position. In Figure 6.1 two examples of a matching result are given for a thoracic scout view and a short-axis cardiac MR-set.

By matching the thorax model to a set of scout views, the same set of geometric transformations required to map the model to the image set can be applied to estimate the position and orientation of the LV long axis. Based on these estimates, the short-axis image volume can be fully automatically defined directly from the scout views, where the three-dimensional angulation of the LV long axis defines the orientation of the image set.

The automated model matching procedure was applied directly to the 20 patient scout views acquired for the manual scan volume definition. This yielded the two parameters required for the short-axis scan planning: an estimated position of the center of gravity of the image volume and the direction of the normal vector for the image planes. In this matching step, no subjective user interaction was required. The number of slices in the automatically defined scanning grid set was set to 13. Computations were per-

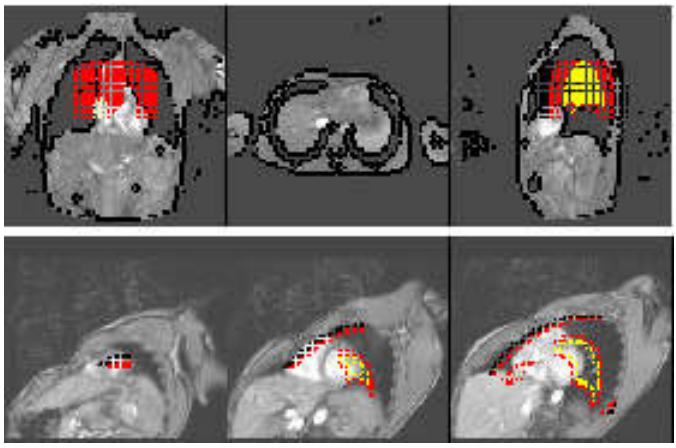

Figure 6.1: Two application examples of a deformable thorax model after fully automatically matching it to two thoracic MR image sets. The dotted boundary strips represent the expected location of the boundaries of the left lung, right lung, diaphragm and epicardial surfaces. The top row shows the model displayed on three orthogonal slices from a thorax scout view consisting of 27 slices. The bottom row displays the result of the direct application of the model matching procedure to a set of short-axis cardiac MR images, displayed on three slice levels in the image set. Click on the images to activate the movies.

formed on a standard Sun Ultrasparc 10 workstation (Sun Microsystems, Mountainview, CA).

In addition to these experiments, the method was applied in practice for two normal subjects by automatically planning the short-axis image planes in a set of the scout views, and acquiring the corresponding short-axis image volumes.

Gold standard denition

The orientation of the geometric long axis at end-diastole was selected as the reference for the orientation of the LV long axis. To calculate this orientation for each image set, the contours of the endocardium were manually drawn in all short-axis cardiac MR-scans at end-diastole. The orientation of the LV long axis in each image set was subsequently calculated by tting a straight line through the contour centroids of the end-diastolic contours using a least squares distance criterion. In Figure 6.2, an example of a reference LV-long axis is given for one of the patient studies.

Denition of accuracy and reproducibility

To dene the best achievable accuracy and to calculate a realistic error margin for the reference long axis, the variation in the LV orientation over the cardiac cycle was calculated. This was estimated by assessing the angle φ_{cycle} between the end-diastolic (ED) and the

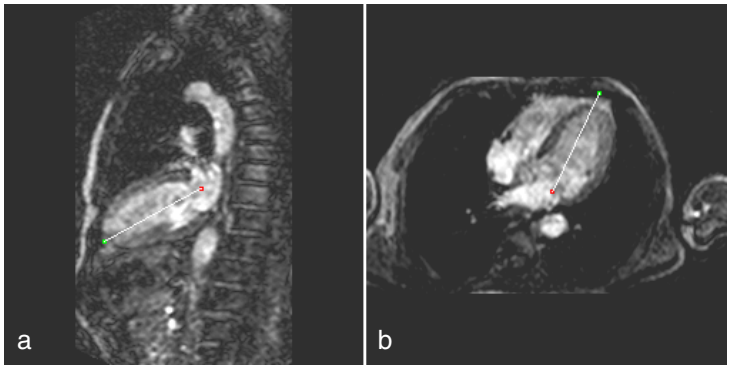

Figure 6.2: Example of a left ventricular long axis, calculated from the LV contours in a short-axis image set. (a) LV long axis projected on a vertical long axis view. (b) LV long axis projected on a 4 chamber view.

end-systolic (ES) geometric LV long axes as determined from the contours in the short-axis images in ED and ES, respectively.

The variabilities introduced in the manual scan planning process were assessed by calculating the angle φ_{manual} between the gold standard LV long axis and the orientation (normal vector) of the manually planned short-axis images (see Figure 6.3). This angle expresses the error introduced by the scanner operator accumulated over all the stages of the manual planning procedure, and provides an indicator for the accuracy by which the LV long axis is determined in routine clinical practice on a standard clinical MR system.

To evaluate the automatically estimated LV orientation against the reference LV long axis orientation, the angle $\varphi_{automatic}$ was calculated between the gold standard LV long axis

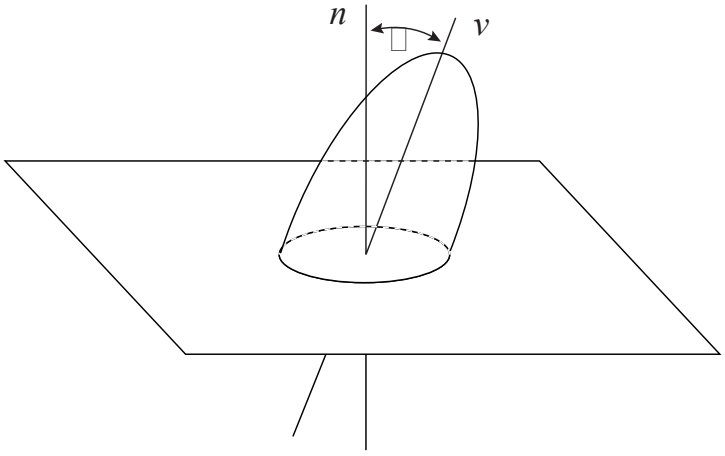

Figure 6.3: To quantitate the errors in both the manual and automatic scan planning procedures, the angle φ between the image normal vector n and the geometric LV long axis v was calculated.

and the automatically estimated LV long axis. This measure represents the deviations in orientation of the automatically defined scanning volumes as compared to the gold standard LV long axis.

6.3 Results

For all twenty patient examinations, the results of the quantitative comparison between the automatically and the manually planned image sets are given in Table 6.1.

Table 6.1 Offset angle $\varphi_{automatic}$ for the automatic procedure, φ_{manual} for the manual procedure, and angle φ_{cycle} between the end-diastolic and end-systolic LV long axes caused by the cardiac contraction

	$\varphi automatic$	$\varphi manual$	$\varphi cycle$
1	9.6	5.3	8.6
2	8.3	13.9	3.6
3	12.4	16.1	6.7
4	12.5	28.9	22.2
5	21.7	5.7	9.2
6	7.6	11.8	6.9
7	5.3	2.2	1.7
8	9.6	9.7	4.4
9	15.6	13.0	8.7
10	5.0	4.6	4.5
11	25.2	3.8	0.2
12	4.6	9.1	11.1
13	19.8	9.3	2.9
14	6.8	8.9	4.7
15	16.3	8.1	0.5
16	7.9	11.1	7.8
17	1.9	7.4	1.4
18	20.1	6.3	6.8
19	22.3	6.7	1.7
20	12.0	11.9	9.0
average	12.2	9.7	6.1
std. dev.	6.8	5.8	5.0

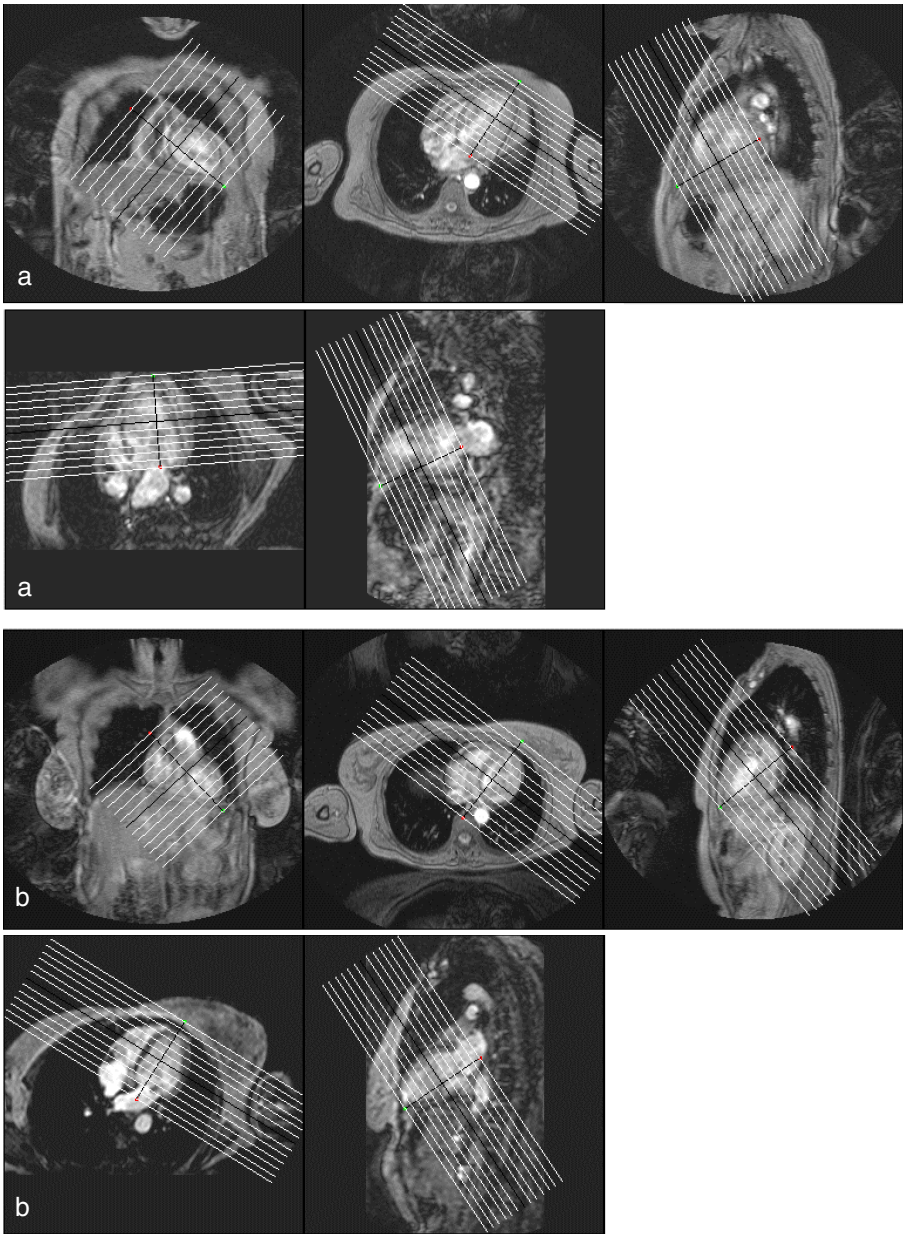

Figure 6.4: Examples of fully automatically planned scanning grids for two patients, a and b. For each patient, the top row displays the scanning grid, projected on three orthogonal slices from the scout data. To visually verify the correctness of the planned image volumes, the grids were also projected on the four-chamber view and the vertical long-axis view respectively (bottom row), which were acquired during the manual scan planning protocol. These images were not used in the model matching procedure.

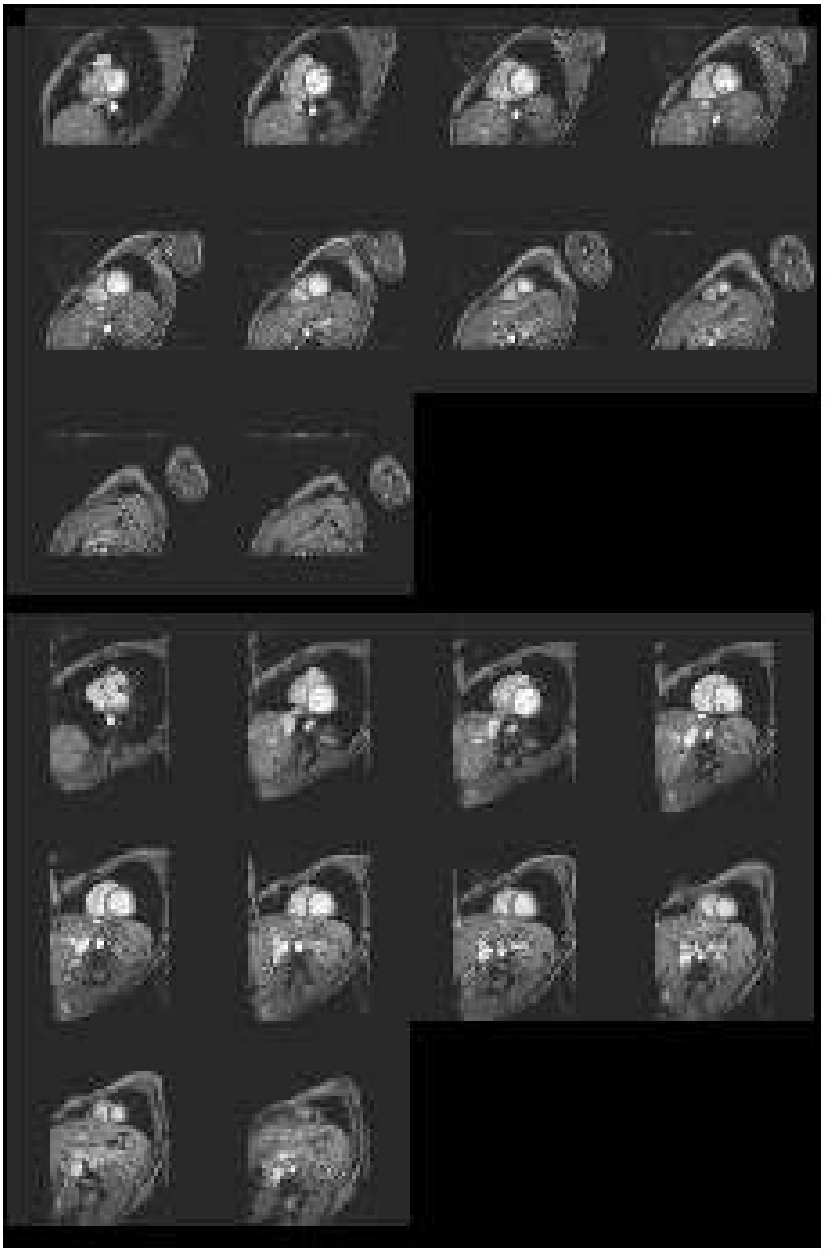

Figure 6.5: Comparison between manually planned short-axis images (top) and automatically planned short-axis images (bottom). Though the slice locations differ slightly, the appearances of the left and right ventricles are highly similar in both image sets. Click on the image to activate the animation.

The angular variations in the orientation of the reference LV long axis over the cardiac cycle φ_{cycle} was on average 6.1 degrees (SD 5.0 degrees, range [0.2-22.2 degrees]). The measured φ_{manual} was on average 9.7 degrees (SD 5.8 degrees, range [2.2-28.9 degrees]), while the angular offset $\varphi_{automatic}$ amounted on average 12.2 degrees (SD 6.8 degrees, range [1.9-25.2] degrees).

In Figure 6.4, two representative examples of fully automatically defined scanning grids resulting from the automated planning procedure are displayed. In Figure 6.5, an example is given of the manually defined short-axis scans as compared to the automatically acquired short-axis images. Computing times required to calculate the scanning parameters for the short-axis image volumes ranged between 3 and 5 minutes for a set of scout views consisting of 27 images.

6.4 Discussion

To accurately analyze left ventricular function from short-axis cardiac MR-images requires that these images are acquired perpendicular to the LV long axis. The purpose of this study was to investigate the feasibility of an automated scan planning method, which automatically provides correct scanning parameters for these short-axis volumes. This method potentially reduces user interaction to a minimum, reduces acquisition time and requires no specialized knowledge to correctly define a short-axis cardiac MR volume. The study quantitatively compares the automated scan planning method with a routinely applied manual scan planning protocol.

Accuracy of manual versus automated scan planning

The manually introduced angle between the short-axis image orientation and the reference LV long axis (φ_{manual}) together with the change in direction of the LV long axis over the cardiac cycle φ_{cycle}) resulted in deviations from the gold standard orientation in an order of magnitude between 2 and 29 degrees. This illustrates that short axis views as planned manually in routine clinical practice may deviate significantly from the optimal view perpendicular to the geometrical LV long axis.

The error in the automated planning method ($\varphi_{automatic}$) varied in a slightly smaller range (between 2 and 25 degrees) as compared to the manual planning procedure. The average angular offset in the automatically planned short-axis volumes amounted to 12.2 degrees, which is comparable to the inaccuracies in the manual scan planning procedure (average 9.7 degrees). In a two-tailed paired samples t-test, this difference was found to be not statistically significant ($p=0.23$). The automated method also demonstrated a comparable standard deviation as the manual scan planning procedure (6.8 degrees versus 5.8 degrees) in the angular offset from the gold standard LV long axis. This difference was statistically non-significant (one tailed F-test, $p=0.49$), and is in the same order of magnitude of the standard deviation in φ_{cycle} (5.0 degrees), which represents the variation in orientation of the LV long axis over the cardiac cycle.

Although the differences in the error distributions of the manual and the automated procedure were found to be statistically non significant, a possible reason for a systematic error in the automated procedure is the fact that the scout views used for the automated scan planning were non-breathheld, whereas the short axis images used to define the gold standard LV orientation were acquired in end-expiration. A change in respiratory status introduces a difference in orientation and position of the heart in the thorax, causing a slight difference between the LV long axis orientation in the scout views and the LV axis in the short-axis image volumes used to define the gold standard LV orientation. Such a systematic offset can possibly be corrected with a correction factor, which would account for the difference in orientation in the LV position over the respiratory cycle. On the other hand, recent advances in MR technology allow breath-held survey acquisitions, which would enable the acquisition of scout views in the same phase of the respiratory cycle as the short-axis MR-images.

Impact of image orientation errors on LV wall measurements

Although in the automatically and manually defined scan definitions the angular offsets range between 2-25 degrees and 2-29 degrees respectively, the impact of angular errors on actual LV wall thickness and thickening measurements is limited due to the fact that an angular offset causes only a slight overestimation of the wall thickness of $(1 / \cos(\varphi)) \times 100\%$. For angles smaller than 18 degrees the error is less than 5%. Using a 2D centerline wall thickness measurement [15], this would lead for the manually planned short-axis images (worst case offset 29 degrees) to a worst case local overestimation of the wall thickness by 14%. For the automated method this worst-case offset (25 degrees) would cause an overestimation of 10%.

Practical considerations and limitations

The automated scan planning method presented here is intended for application in a supervised manner. In this study, we eliminated any user interaction to investigate the accuracy and reliability of the method. The results of this study indicate that without any user interaction, the worst case angular offset from the geometric LV long axis amounts to 25 degrees, with an average of 12 degrees. However, it is possible to enable user interaction by visualizing the calculated scan volume on the scout image sets and enabling the scanner operator to intervene. Based on the results from this study, it is expected that such user interaction is not required in 90% of the cases.

In the present study the number of slices in the short axis image volume was fixed; as a result a few redundant slices, which did not contain any LV, were included in some cases. In practice, this parameter may be adjusted manually if required. In our current work, we are focusing on the automated assessment of this and a number of other scanning parameters required for different cardiac function protocols, such as navigator position for non-breathheld protocols, and location of the aortic arch for the acquisition of velocity encoded aortic flow images.

The automated scan planning method has been developed to work on current standard MR hardware. A recent advance in MR acquisition technology is the development of real-time MR scanners, which allow an interactive scan planning of the short-axis image plane. This may significantly reduce the time required to plan the short-axis image planes. However, interactive scan planning, which is still in a developmental stage, remains subjective and does not provide a uniform means to determine the optimal short-axis view independent of observer experience and interpretation.

The time required for the automated scan planning procedure currently amounts to 5-7 minutes, including the acquisition of the scout views (2 minutes) and the calculation of the scan volume acquisition parameters (3-5 minutes). In general, this is only slightly faster than the time required for the manual scan planning procedure, particularly because the necessity to acquire supporting long axis views is eliminated. However, we foresee two possibilities to further speed up the automated process. Firstly, the rapid evolution of computer hardware will enable us to further shorten the automated matching procedure. Secondly, initial experiments have been performed by applying the automated model matching procedure to only a subset of the scout image volume. By selecting a subset of the scout images, for instance every other image or every third image, the planning procedure can be shortened by a factor of 2-4 with comparable accuracy. These two factors may potentially reduce the time to automatically plan the short-axis image volume to 3 minutes including the scout scanning.

6.5 Conclusions

This study investigated the feasibility of an observer independent scan planning method for short-axis cardiac MR-images. The automated planning procedure was found to perform with comparable accuracy as the manual scan planning in routine clinical practice. Currently, the time for the automated planning protocol is slightly shorter than for the manual scan planning, mainly because no additional long axis support scans were required. However, the main advantage of the automated method over the manual planning procedure, is the fact that it provides a uniform, observer independent planning approach requiring no expert knowledge, while yielding images of comparable quality as manually planned images.

6.6 References

1. Yang PC, Kerr AB, Liu AC, et al. New real-time interactive cardiac magnetic resonance imaging system complements echocardiography. J Am Coll Cardiol 1998; 32:2049-2056.
2. Shapiro EP, Rogers WJ, Beyar R. Determination of left ventricular mass by magnetic resonance imaging in hearts deformed by acute infarction. Circulation 1989; 47:706-711.
3. Haag UJ, Maier SE, Jakob M, et al. Left ventricular wall thickness measurements by magnetic resonance: a validation study. Int J Cardiac Imag 1991; 7:31-41.

4. Azhari H, Sideman S, Weiss JL, et al. Three-dimensional mapping of acute ischemic regions using MRI: wall thickening versus motion analysis. Am J Physiol 1990; 259:H1492-H1503.
5. van Rugge FP, van der Wall EE, Spanjersberg SJ, et al. Magnetic resonance imaging during dobutamine stress for detection of coronary artery disease; quantitative wall motion analysis using a modification of the centerline method. Circulation 1994; 90:127-138.
6. van der Geest RJ, de Roos A, van der Wall EE, Reiber JHC. Quantitative analysis of cardiovascular MR images. Int J Cardiac Imag 1997; 13:247-258.
7. van der Geest RJ, Buller VGM, Jansen E, et al. Comparison between manual and automated analysis of left ventricular volume parameters from short axis MR images. J Comput Assist Tomogr 1997; 21:756-765.
8. Lamb HJ, Singleton RR, van der Geest RJ, Pohost GM, de Roos A. MR imaging of regional cardiac function: Low-pass filtering of wall thickness curves. Magn Reson Med 1995; 34:498-502.
9. Holman ER, Vliegen HW, van der Geest RJ, et al. Quantitative analysis of regional left ventricular function after myocardial infarction in the pig assessed with cine magnetic resonance imaging. Magn Reson Med 1995; 34:161-169.
10. Pattynama PMT, Lamb HJ, van der Velde EA, van der Wall EE, de Roos A. Left ventricular measurements with cine and spin-echo MR imaging: a study of reproducibility with variance component analysis. Radiology 1993; 187:261-268.
11. Lamb HJ, Doornbos J, van der Velde EA, Kruit MC, Reiber JHC, de Roos A. Echo-panar MRI of the heart on a standard sytem: validation of measurement of left ventricular function and mass. J Comp Assist Tomogr 1996; 20:942-949.
12. Lelieveldt BPF, van der Geest RJ, Reiber JHC. Automated model driven localization of the heart and lung surfaces in thoracic MR images. Computers in Cardiology 1998; 25:9-12.
13. Lelieveldt BPF, van der Geest RJ, Ramze Rezaee M, Bosch JG, Reiber JHC. Anatomical model matching with fuzzy implicit surfaces for segmentation of thoracic volume scans. IEEE T Med Imaging 1999; 18:218-230.
14. Lelieveldt BPF, Sonka M, Bolinger L, et al. Anatomical modeling with fuzzy implicit surfaces: application to automated localization of the heart and lung surfaces in thoracic MR Images. In: vol.1613 of Lecture Notes in Computer Science, proc. Information Processing in Medical Imaging, Visegrad, Hungary, 1999; 400-405.
15. Sheehan FH, Bolson EL, Dodge HT, Mathey DG, Schofer J, Woo HK. Advantages and applications of the centerline method for characterizing regional ventricular function. Circulation 1986; 74:293-305.